Generalized hydrodynamics and shock waves

Mazen Al-Ghoul and Byung Chan Eu*
Department of Chemistry, McGill University, 801 Sherbrooke Street West, Montreal, Quebec, Canada H3A 2K6
(Received 6 December 1996; revised manuscript received 3 March 1997)

In this paper, the generalized hydrodynamic equations are applied to calculate the shock profiles, shock widths, and calortropy production (energy dissipation) for a Maxwell and variable hard sphere gas. Shock solutions are shown to exist for all Mach numbers (N_M) studied, ranging up to $N_M=10$, but this upper Mach number can be in principle extended to infinity. This is in contrast to the Grad moment equation method [H. Grad, Commun. Pure Appl. Math, **5**, 257 (1952)] which does not admit shock solutions for $N_M \geqslant 1.65$ and to the method of Anile and Majorana [A. M. Anile and A. Majorana, Meccanica **16**, 149 (1982)] and Weiss [W. Weiss, Phys. Rev. E **52**, R5760 (1995)] who also used moment equations and found the shock solutions do not exist for $N_M \geqslant 2.09$ and $N_M \geqslant 1.887$, respectively. The difference of the present theory from the aforementioned theories lies in the closure relations used for higher-order moments. The nonlinear factor in the dissipation terms in the flux evolution equations of generalized hydrodynamics significantly contributes to producing the shock width increasing with the Mach number. The results calculated are comparable with the Monte Carlo simulation results and the results by various closures of the Mott-Smith method. The present method is also applied to calculate the experimental shock widths for argon and found to give results in good agreement with experiments. The energy dissipation is shown to increase with N_M as $(N_M-a)^{\alpha}$, where a and α are positive constants. [S1063-651X(97)07809-4]

PACS number(s): 47.40.Hg, 47.40.Ki

I. INTRODUCTION

Investigations on shock structures have been made in a number of approaches in the past. They include the Navier-Stokes theory [1–3], which historically precedes other approaches that include the kinetic theory methods and Monte Carlo and molecular dynamic simulation methods [4–10]. The latter group of methods may be regarded as molecular theories of shock structures since they are essentially based on either a kinetic equation or molecular equations of motion for the particles in the system. In the kinetic theory methods used for the study of shock structures, there are several approaches making use of the higher-order Chapman-Enskog solutions, namely, the Burnett and super-Burnett solutions [11–13], the bimodal distribution function method of Mott-Smith [14] and its generalizations [15–22], and Grad's moment method [23–26]. These molecular theoretic approaches have been taken because of the failure of the Navier-Stokes theory for shock structures for gases, which tends to fail in the hypersonic regime beyond the Mach number in the neighborhood of 1.5. When the Burnett- and super-Burnett-order solutions of the Boltzmann equations are implemented with the steady-state governing equations, they generally fail to give adequate solutions for shock wave problems, but the recent work by Fiscko and Chapman [13] shows that reasonable results can be obtained for shock structures if some terms in the Burnett-order solutions are simply neglected and the time-dependent governing equations are solved instead of the conventional steady-state governing equations used for steady shock wave problems. The precise reason is not clear why the time-dependent governing equations yield shock solutions whereas the steady-state governing equations do not. In any case, it must be noted that if the Burnett- and super-Burnett-order solutions are examined from the viewpoint of the H theorem demanded by the Boltzmann equation, they are inconsistent with it since they generally yield a nonpositive Boltzmann entropy production. Perhaps, the neglected terms mentioned earlier in connection with the work by Fiscko and Chapman may be responsible for restoring the consistency with the H theorem. The Mott-Smith method is a nonsystematic method based on a kinetic equation, for example, the Boltzmann equation, although it gives adequate numerical results for shock structures and profiles which can vary with the moments taken to construct a bimodal distribution function. Grad [23] made a critique of this feature and formulated a theory by means of moment equations derived from the Boltzmann equation, but his thirteen moment equations failed to give shock wave solutions as the Mach number exceeds the critical value of $N_M=1.65$. Since his moment equations form an open set, Grad had to introduce closure relations for moments in order to get the thirteen moment equations. We will elaborate on his closures later in this paper. It must be noted that there is no unique way of introducing the closures to the Grad moment equations at present. Since it is credible to imagine that the moment sequence converges, the failure of the Grad approach inspired further research by a number of authors [24–26] who have taken a larger number of moments or fashioned the moment equations in supposedly more adequate forms. These stratagems did not succeed in removing the critical Mach number problem of the Grad approach, and rather complicated moment equations which become quite difficult to solve do not increase the critical Mach number significantly as evident from the values known in the literature: $N_M=1.85$ in the case of Holway, $N_M=2.09$ in the case of Anile and Majo-

*Also at Dept. of Physics and Centre for the Physics of Materials, McGill University, Montreal, Quebec, Canada H3A 2K6. Electronic address: Eu@OMC.Lan.McGill.ca

rana, and, most recently, $N_M = 1.887$ by Weiss who used 21 moments. Therefore, the Grad method of closure, which is achieved by expressing the truncated (higher-order) moments in terms of the lower-order moments retained, does not yield a set of continuum theory governing equations which yield shock solutions for all values of Mach number as does the Navier-Stokes theory, albeit poorly. This difficulty of the Grad moment equations derived from the Boltzmann equation therefore is a challenge for the shock wave problem, and it is important to overcome it since the Grad approach provides a simpler set of macroscopic equations than the Chapman-Enskog method and hence is potentially more useful for formulating a macroscopic theory of irreversible processes. In fact, it can serve as the starting point to formulate a theory of irreversible processes as shown in Ref. [27] which is a theory aimed to generalize the classical theory of linear irreversible thermodynamics [28]. Therefore, the aforementioned difficulty in connection with the closure poses a serious conceptual problem for the theory of irreversible processes based on the moment evolution equations. Such a theory ought to be able to account adequately for shock wave phenomena. Therefore, the shock wave problem can serve as a touchstone for both irreversible thermodynamics and the approximate solution methods in the kinetic theory of gases, and thus is an important problem to consider. As will be shown, the closure relations hold the key to the resolution of the problem and with suitable closures we obtain a well-behaved set of relatively simple governing equations for flow which provide reliable and accurate numerical results for shock phenomena.

In this paper, we study the question from the viewpoint of the generalized hydrodynamics formulated in the nonequilibrium ensemble method [29] and the version of extended irreversible thermodynamics [30] which is given statistical mechanical foundations with the former. Since the generalized hydrodynamic equations employed are basically the moment evolution equations, one can wonder if there is any basis to hope that they will provide us with an adequate solution to the problem. The answer is in the affirmative, since the closure relations used for the constitutive equations in this work make a crucial difference from those used by Grad [23] and others [24–26]. Furthermore, the applications of the steady constitutive equations subjected to the closure relations used here have produced some results which are in quantitative agreement with experimental rheological data [31–36]. Such agreements have been rather encouraging and we would like to show that similarly encouraging results can be obtained for shock wave problems. In this work, we will only consider a one-dimensional steady shock wave problem.

The present paper is organized as follows. In Sec. II, we present the governing equations for the one-dimensional shock problem which are derived from the generalized hydrodynamic equations presented in the previous works [27,29,30] related to the nonequilibrium ensemble method and extended irreversible thermodynamics formulated by one of us. The new closure relations are explicitly presented. In Sec. III, these governing equations are examined for shock solutions. In Sec. IV, the governing equations are solved for shock profiles and shock widths for a Maxwell gas. The inverse shock widths calculated by the present theory for a Maxwell gas are compared with the Monte Carlo simulation results, the results by the Mott-Smith method and its variants, and the Navier-Stokes theory results. Inverse shock widths are also calculated by using a variable hard sphere model and compared with experimental data on argon. They are found to be in good agreement with experiments. The global calortropy production [29] is a measure of energy dissipation from a useful to a less useful form of energy in irreversible processes. We study its Mach number dependence. Section V is for discussion and conclusion.

II. GOVERNING GENERALIZED HYDRODYNAMIC EQUATIONS

We assume that flow is in the direction of the x coordinate. Since we are interested in a steady shock wave, the governing balance equations for mass, momentum, and energy are time independent. They are in the form

$$\frac{d}{dx}\,\rho u = 0, \tag{1}$$

$$\frac{d}{dx}\,(\rho u^2 + p + \Pi_{xx}) = 0, \tag{2}$$

$$\frac{d}{dx}\left[\rho u\left(\mathcal{E} + \frac{1}{2}\,u^2\right) + u(p + \Pi_{xx}) + Q_x\right] = 0, \tag{3}$$

where ρ is the mass density, u is the fluid velocity, p is the pressure, Π_{xx} is the xx component of the shear stress, $\mathcal{E}$ is the internal energy density, and Q_x is the x component of the heat flux. We note that in one-dimensional flow geometry for the present problem

$$[\boldsymbol{\nabla}\mathbf{u}]_{xx} = \frac{2}{3}\,\partial_x u. \tag{4}$$

These balance equations are supplemented by the evolution equations for Π_{xx} and Q_x within the framework of the first thirteen moments. The evolution equation for the stress tensor and heat flux [27] are

$$\rho\,\frac{d\hat{\boldsymbol{\Pi}}}{dt} = -\boldsymbol{\nabla}\cdot\boldsymbol{\psi}_2 - 2p[\boldsymbol{\nabla}\mathbf{u}]^{(2)} - 2[\boldsymbol{\Pi}\cdot\boldsymbol{\nabla}\mathbf{u}]^{(2)} - \frac{p}{\eta_0}\,\boldsymbol{\Pi} q(\kappa), \tag{5}$$

$$\rho\,\frac{d\hat{\mathbf{Q}}}{dt} = -\boldsymbol{\nabla}\cdot\boldsymbol{\psi}_3 - p\hat{C}_p T\boldsymbol{\nabla}\,\ln T - \boldsymbol{\Pi}\cdot\boldsymbol{\nabla}\hat{h} + \boldsymbol{\nabla}(p\boldsymbol{\delta} + \boldsymbol{\Pi})\cdot\hat{\boldsymbol{\Pi}}$$

$$-\mathbf{Q}\cdot\boldsymbol{\nabla}\mathbf{u} - \frac{p\hat{C}_p T}{\lambda_0}\,\mathbf{Q} q(\kappa), \tag{6}$$

where $\boldsymbol{\delta}$ is the unit second-rank tensor, $d/dt = \partial/\partial t + \mathbf{u}\cdot\boldsymbol{\nabla}$ is the substantial time derivative, and $\boldsymbol{\psi}_2$ and $\boldsymbol{\psi}_3$ are higher-order moments which are defined, in the case of a dilute monatomic gas, by the statistical formulas

$$\boldsymbol{\psi}_2 = \langle m\mathbf{C}[\mathbf{CC}]^{(2)} f(\mathbf{C};t)\rangle,$$

$$\boldsymbol{\psi}_3 = \left\langle \frac{1}{2}\,mC^2\mathbf{CC} f(\mathbf{C};t)\right\rangle, \tag{7}$$

with $\mathbf{C}$ denoting the peculiar velocity and $f(\mathbf{C};t)$ the nonequilibrium distribution function obeying a kinetic equation, say, the Boltzmann equation. The symbol $[\nabla\mathbf{u}]^{(2)}$ stands for the traceless symmetric part of $\nabla\mathbf{u}$. Other symbols are as follows: $\mathbf{\Pi}$ denotes the traceless symmetric part of pressure tensor $\mathbf{P}$, $\hat{\mathbf{\Pi}}=\mathbf{\Pi}/\rho$; $\mathbf{Q}$ is the heat flux, $\hat{\mathbf{Q}}=\mathbf{Q}/\rho$; $\hat{C}_p$ is the specific heat per mass at constant pressure; $\hat{h}=\hat{C}_pT$ is the enthalpy per mass; η_0 and λ_0 are the Chapman-Enskog viscosity and thermal conductivity [37], respectively; and $q(\kappa)$ is a nonlinear factor defined by

$$q(\kappa)=\frac{\sinh\kappa}{\kappa}, \tag{8}$$

where

$$\kappa=\frac{(mk_BT)^{1/4}}{\sqrt{2}pd}\left(\frac{1}{2\eta_0}\,\mathbf{\Pi}:\mathbf{\Pi}+\frac{1}{\lambda_0}\,\mathbf{Q}\cdot\mathbf{Q}\right)^{1/2}. \tag{9}$$

Here d denotes the diameter of the molecule and m is the molecular mass. In Eq. (6), we have omitted a term related to a third-rank tensor, namely, $\langle m\mathbf{CCC}f(\mathbf{C};t)\rangle:\nabla\mathbf{u}$ in accordance with the spirit of the thirteen moment method. Furthermore, this term, even if taken into account, would not change the basic conclusion of this work; it will merely add to the second term from the last in Eq. (6) if it is expressed in terms of lower-order moments. The higher-order moments $\boldsymbol{\psi}_2$ and $\boldsymbol{\psi}_3$ obey their own evolution equations. Therefore, the evolution equations (5) and (6) are the leading members of an open set of moment equations. It is usually closed by expressing $\boldsymbol{\psi}_2$ and $\boldsymbol{\psi}_3$ in the lower-order moments, namely, $\mathbf{\Pi}$ and $\mathbf{Q}$ as well as the conserved moments ρ, $\mathbf{u}$, and $\mathcal{E}$. Within the first thirteen moment approximation $\boldsymbol{\psi}_2$ is proportional to $\mathbf{Q}$, whereas $\boldsymbol{\psi}_3$ is given in terms of $\mathbf{\Pi}$. Such closure relations give rise to partial differential equations for $\mathbf{\Pi}$ and $\mathbf{Q}$, which form the governing equations for shock wave problems in the approaches [24–26] based on the moment equations following Grad [23]. We have earlier mentioned that such approaches do not yield shock solutions for the Mach number beyond a critical value. We propose a different set of closures in this paper.

We take the following closure relations for $\boldsymbol{\psi}_2$ and $\boldsymbol{\psi}_3$ appearing in the moment evolution equations for $\mathbf{\Pi}$ and $\mathbf{Q}$:

$$\boldsymbol{\psi}_2=\boldsymbol{\psi}_3=\mathbf{0}. \tag{10}$$

This set of closure relations is different from those taken in Grad's theory of solution for the Boltzmann equation and various existing variants of it, but there is no *a priori* reason to disfavor the present closure relations over those which expand $\boldsymbol{\psi}_2$ and $\boldsymbol{\psi}_3$ in $\mathbf{Q}$ and $\mathbf{\Pi}$ as well as density and temperature, since Grad's closure does not have a theoretical justification either. It is worthwhile to examine this closure relation a little more closely in order to see its difference from Grad's closure. In Grad's closure using the thirteen moments, the distribution function $f(\mathbf{C};t)$ is written as

$$f(\mathbf{C};t)=f_0\left(1+A_p:[\mathbf{CC}]^{(2)}+A_q\cdot\frac{1}{2}\,mC^2\mathbf{C}\right), \tag{11}$$

where f_0 is the local equilibrium distribution function and the coefficients A_p and A_q are, respectively, proportional to $\mathbf{\Pi}$ and $\mathbf{Q}$. It must be noted that in this approximation the moments higher than $\mathbf{\Pi}$ and $\mathbf{Q}$ (e.g., the third and fourth rank tensors) are set equal to zero. Therefore, we find

$$\boldsymbol{\psi}_2=\frac{4}{5}\,\mathbf{T}\cdot\mathbf{Q},\quad \boldsymbol{\psi}_3=\frac{5p^2}{2\rho}\,\boldsymbol{\delta}+\frac{7p}{2\rho}\,\mathbf{\Pi}, \tag{12}$$

where $\mathbf{T}$ is an isotropic fourth-rank tensor defined by [27]

$$\mathbf{T}_{ijkl}=\frac{1}{2}\,(\delta_{ik}\delta_{jl}+\delta_{il}\delta_{jk})-\frac{1}{3}\,\delta_{ij}\delta_{kl}.$$

On the other hand, in the present theory the distribution function is written in an exponential form in terms of tensor Hermite polynomials $\mathcal{H}^{(k)}(\mathbf{w})$ $(k\geqslant 0)$ of reduced peculiar velocity $\mathbf{w}=\sqrt{m/k_BT}\mathbf{C}$ as in

$$f(\mathbf{C};t)=\exp\left[-\frac{1}{k_BT}\left(\frac{1}{2}\,mC^2+\sum_{k\geqslant 1}X_k\mathcal{H}^{(k)}(\mathbf{w})-\mu\right)\right], \tag{13}$$

where μ is the normalization factor and X_k are the generalized potentials which depend only on macroscopic variables such as $\mathbf{\Pi}$ and $\mathbf{Q}$. Then, it is possible to show that

$$\boldsymbol{\psi}_2=\sqrt{k_BT/m}[\Theta_3+\Theta_1\boldsymbol{\delta}],$$

$$\boldsymbol{\psi}_3=\sqrt{k_BT/m}[\Theta_4+\Theta_2\boldsymbol{\delta}], \tag{14}$$

where Θ_3, etc., are moments defined by

$$\Theta_k=\langle\mathcal{H}^{(k)}(\mathbf{w})f(\mathbf{C};t)\rangle. \tag{15}$$

Therefore, the closures in Eq. (10) imply that in the present theory the higher-order-moments Θ_3, Θ_4, etc., are expressed as follows:

$$\Theta_3=-\Theta_1\boldsymbol{\delta}=0,\quad \Theta_4=-\Theta_2\boldsymbol{\delta}=-\mathbf{\Pi}\boldsymbol{\delta}. \tag{16}$$

Note that $\Theta_2=\mathbf{\Pi}$ since $\mathcal{H}^{(2)}(\mathbf{w})=\mathbf{ww}-\boldsymbol{\delta}$, and $\Theta_1=0$. These results should be examined in the context of Grad's expansion (11) for f where the third-, fourth-,..., rank tensor terms are set equal to zero. Since both the Grad's and the present closure express the higher-order moments in terms of lower-order moments, the same idea is used but their manners of implementation are different. However, despite the same idea the different manners of implementation make their implications greatly different as we will see in the case of shock structures obtained.

With the closure relations (10) the constitutive equations are given by

$$\rho\,\frac{d\hat{\mathbf{\Pi}}}{dt}=-2p[\nabla\mathbf{u}]^{(2)}-2[\mathbf{\Pi}\cdot\nabla\mathbf{u}]^{(2)}-\frac{p}{\eta_0}\,\mathbf{\Pi}q(\kappa), \tag{17}$$

$$\rho \frac{d\hat{\mathbf{Q}}}{dt} = -p\hat{C}_p T\boldsymbol{\nabla} \ln T - \boldsymbol{\Pi}\cdot\boldsymbol{\nabla}\hat{h} + \boldsymbol{\nabla}(p\boldsymbol{\delta}+\boldsymbol{\Pi})\cdot\hat{\boldsymbol{\Pi}} - \mathbf{Q}\cdot\nabla\mathbf{u} - \frac{p\hat{C}_p T}{\lambda_0}\mathbf{Q}q(\kappa). \tag{18}$$

We have shown in a number of studies [27,31–36] on nonlinear transport coefficients that the constitutive equations (19) and (20) give rise to sufficiently accurate nonlinear transport coefficients and particularly non-Newtonian viscosities in comparison with experiments. On the strength of this finding, we take the closure relations in Eq. (10) and show their effectiveness for the shock wave problem. We are thereby able to formulate a continuum hydrodynamic theory of shock waves which provides shock solutions beyond the critical Mach numbers mentioned earlier in connection with the moment method approaches. Based on the examination of the direction field for the governing equations in the present theory, it will become evident that shock solutions should exist for all Mach numbers.

The nonconserved variables such as $\boldsymbol{\Pi}$ and $\mathbf{Q}$ vary on a faster time scale than the conserved variables such as the density, energy (or temperature), and momentum (or fluid velocity). Therefore, on the time scale of variation in the conserved variables the nonconserved variables have already reached their steady state, and it can be shown [27] that the following approximate constitutive equations hold for $\boldsymbol{\Pi}$ and $\mathbf{Q}$:

$$-2p[\boldsymbol{\nabla}\mathbf{u}]^{(2)} - 2[\boldsymbol{\Pi}\cdot\boldsymbol{\nabla}\mathbf{u}]^{(2)} - \frac{p}{\eta_0}\boldsymbol{\Pi}q(\kappa) = \mathbf{0}, \tag{19}$$

$$-p\hat{C}_p T\boldsymbol{\nabla} \ln T - \boldsymbol{\Pi}\cdot\boldsymbol{\nabla}\hat{h} + \boldsymbol{\nabla}(p\boldsymbol{\delta}+\boldsymbol{\Pi})\cdot\hat{\boldsymbol{\Pi}} - \mathbf{Q}\cdot\boldsymbol{\nabla}\mathbf{u} - \frac{p\hat{C}_p T}{\lambda_0}\mathbf{Q}q(\kappa) = \mathbf{0}. \tag{20}$$

This approximation is called the adiabatic approximation. The utility of this approximation has successfully been tested for a number of flow problems [27]. We use these constitutive equations in the present work for shock waves.

In the case of flow geometry for the present problem, the steady-state constitutive equations for Π_{xx} and Q_x under the closure relations mentioned are obtained from Eq. (5) and Eq. (6) as follows:

$$\frac{p}{\eta_0}\Pi_{xx}q(\kappa) + \frac{4}{3}\Pi_{xx}\partial_x u + \frac{4}{3}p\partial_x u = 0, \tag{21}$$

$$\frac{\hat{h}_p}{\lambda_0}Q_x q(\kappa) + Q_x\partial_x u + \Pi_{xx}u\partial_x u + \hat{h}(p+\Pi_{xx})\partial_x \ln T = 0. \tag{22}$$

Equations (21) and (22) are partial differential equations for velocity component u and temperature T. We emphasize that there do not appear partial derivatives of Π_{xx} and Q_x in these equations owing to the closure relations taken.

Integration of the balance equations (1)–(3) yields

$$\rho u = M, \tag{23}$$

$$\rho u^2 + p + \Pi_{xx} = P, \tag{24}$$

$$\rho u\left(\mathcal{E} + \frac{1}{2}u^2\right) + u(p+\Pi_{xx}) + Q_x = Q, \tag{25}$$

where M, P, and Q are integration constants with the dimension of momentum per volume, momentum flux per volume, and energy flow per volume, respectively. These equations are also supplemented by the equation of state and the caloric equation of state

$$p = \rho\mathcal{R}T,$$

$$\mathcal{E} = \frac{3}{2}\mathcal{R}T, \tag{26}$$

where $\mathcal{R}$ is the gas constant per mass. Let us define dimensionless variables

$$v = MuP^{-1}, \quad \theta = M^2\mathcal{R}TP^{-2},$$

$$\sigma = \Pi_{xx}P^{-1}, \quad \phi = pP^{-1},$$

$$r = P\rho M^{-2}, \quad \varphi = Q_x Q^{-1},$$

$$\xi = xl^{-1}, \quad \alpha = MQP^{-2}. \tag{27}$$

The length scale is provided by the mean free path l defined with the upstream momentum per volume, $M = \rho_1 u_1$, where the subscript 1 refers to the upstream. The downstream will be designated by subscript 2. The upstream mean free path is defined by

$$l = \frac{\eta_{01}}{M}, \tag{28}$$

where η_{01} is the upstream Newtonian viscosity at the upstream temperature T_1. The transport coefficients η_0 and λ_0 are reduced with respect to the upstream transport coefficients η_{01} and λ_{01}, respectively:

$$\eta^* = \frac{\eta_0}{\eta_{01}}, \quad \lambda^* = \frac{\lambda_0}{\lambda_{01}}. \tag{29}$$

With these reduced variables we cast Eqs. (23)–(26) in the forms

$$\phi = r\theta,$$

$$rv = 1,$$

$$rv^2 + \phi + \sigma = 1,$$

$$rv^3 + 5\phi v + 2\sigma v + 2\alpha\varphi = \alpha. \tag{30}$$

From these equations and on reducing constitutive equations (21) and (22) we obtain the following five equations;

$$\phi v = \theta, \tag{31}$$

$$v + \phi + \sigma = 1, \tag{32}$$

$$v^2 + 5\theta + 2\sigma v + 2\alpha\varphi = \alpha, \tag{33}$$

$$\frac{1}{\eta^*}\,\phi\sigma q(\kappa)+\frac{4}{3}\,\sigma\partial_\xi v+\frac{4}{3}\,\phi\partial_\xi v=0, \tag{34}$$

$$\frac{\alpha\beta}{\lambda^*}\,\theta\varphi q(\kappa)+(\alpha\varphi+v\sigma)\partial_\xi v+\frac{5}{2}\,\theta(\phi+\sigma)\partial_\xi \ln\,\theta=0. \tag{35}$$

Here the new dimensionless parameter β is defined by

$$\beta=\frac{5}{3\theta_1}\,N_{\rm Pr} \tag{36}$$

with θ_1 denoting the reduced upstream temperature and the Prandtl number defined with the upstream quantities $N_{\rm Pr}=\hat{C}_p T_1\eta_{01}/\lambda_{01}$. Since the reduction scheme used here is slightly different from that in the literature [3,23], it is useful to explain it, especially, with regard to the appearance of the dimensionless number β in Eq. (35). On multiplication of the mean free path l, the first term in Eq. (22), apart from the nonlinear factor $q(\kappa)$, can be reduced as follows:

$$l\,\frac{\hat{h}p}{\lambda_0}\,Q_x=\frac{5\tau\phi\varphi}{2\lambda^*}\cdot\frac{lP^3Q}{\lambda_{01}M^2},$$

where the second factor on the right can be written as

$$\frac{lP^3Q}{\lambda_{01}M^2}=\frac{\eta_{01}}{\lambda_{01}}\cdot\frac{P^3Q}{M^3}=\frac{2N_{\rm Pr}}{5\theta_1}\cdot\alpha\cdot\frac{P^2}{M^2}.$$

The second equality in the equation above follows on making use of the definition of Prandtl number and the reduced temperature. Finally, we obtain

$$l\,\frac{\hat{h}p}{\lambda_0}\,Q_x=\frac{\alpha\beta\tau\phi\varphi}{\lambda^*}\cdot\frac{P^2}{M^2}$$

and Eq. (35) follows on dividing the equation with P^2M^{-2} and use of the definition of β in Eq. (36). The argument κ in the nonlinear factor $q(\kappa)$ is given by the formula

$$\kappa=4(2\gamma_0)^{-1/4}(5cN_M)^{-1/2}\left(\frac{\theta}{\theta_1}\right)^{1/4}\frac{1}{\phi\sqrt{\eta^*}}\times\left(\phi^2+\frac{8}{15f\theta}\,\alpha^2\varphi^2\right)^{1/2}, \tag{37}$$

where

$$c=\frac{l}{l_h},\quad f=\frac{4m\lambda_{01}}{15k_BT_1\eta_{01}} \tag{38}$$

with l_h denoting the mean free path for hard spheres in terms of the hard sphere viscosity $l_h=\eta_{01}(\text{hard sphere})/M$. In the case of a Maxwell gas, $f=1$ and

$$c=\frac{16}{15\sqrt{2\pi}A_2(5)}\,\sqrt{\frac{\theta_1}{E_d}},$$

where $A_2(5)=0.436$ and

$$E_d=\frac{V_m}{4md^4}\cdot\frac{M^2}{P^2},$$

which is the reduced Maxwell potential energy of potential strength V_m for two hard spheres of radius $d/2$ at contact. This reduced potential energy is set equal to unity by suitably choosing the reduction parameters M and P. Therefore, for Maxwell molecules with E_d so taken we obtain

$$\kappa=\left(\frac{3\pi}{5}\right)^{1/4}\left(\frac{3A_2(5)}{N_M}\right)^{1/2}\frac{1}{\phi\theta^{1/4}}\left(\sigma^2+\frac{8}{15\theta}\,\alpha^2\varphi^2\right)^{1/2}. \tag{39}$$

We note that the parameter α is related to the upstream Mach number as follows:

$$N_M=\sqrt{\frac{1+(1/5)\mu}{1-(1/3)\mu}}, \tag{40}$$

where

$$\mu=\sqrt{25-16\alpha}. \tag{41}$$

The parameter μ ranges from 0 to 3 which yields $N_M=\infty$. Note that the upstream Mach number can be equivalently defined by

$$N_M=\frac{v_1}{\sqrt{\gamma_0\theta_1}},$$

where γ_0 is the polytropic ratio $\gamma_0=C_p/C_v$.

To determine the boundary conditions on v, ϕ, and θ, we observe that $\sigma\to0$ and $\varphi\to0$ as $\xi\to\pm\infty$. Equations (34) and (35) are identically satisfied in the limits if v and θ become independent of ξ at the boundaries. Therefore, as $\xi\to\pm\infty$

$$\sigma,\varphi\to0, \tag{42}$$

$$\theta=\phi v, \tag{43}$$

$$v+\phi=1, \tag{44}$$

$$v^2+5\theta=\alpha. \tag{45}$$

The solutions of Eqs. (43)–(45) are

$$v=\frac{1}{8}\,(5\pm\mu), \tag{46}$$

$$\phi=\frac{1}{8}\,(3\mp\mu), \tag{47}$$

$$\theta=\frac{1}{64}\,(15\mp2\mu-\mu^2). \tag{48}$$

The upper sign is for the upstream and the lower sign is for the downstream. These solutions provide the boundary conditions at the upstream and downstream. They also imply that the reduced density is given by

$$r=\frac{8}{5\pm\mu}. \tag{49}$$

With the help of Eqs. (31)–(33) the differential equations (34) and (35) may be cast into the following forms:

$$\frac{dv}{d\xi}=\frac{3\theta(v^2-v+\theta)}{4\eta^* v^2(1-v)}\,q(\kappa), \tag{50}$$

$$\frac{d\theta}{d\xi}=-\frac{\theta}{5v^2(1-v)^2}\left[\frac{\beta\theta v(1-v)(\alpha+v^2-2v-3\theta)}{\lambda^*}+\frac{3(v^2-v+\theta)(\alpha-v^2-5\theta)}{4\eta^*}\right]q(\kappa). \tag{51}$$

These governing equations for shock profiles are solved subject to the boundary conditions in Eqs. (46)–(48). These equations generalize the governing equations in the Navier-Stokes theory as will be discussed presently.

III. SHOCK SOLUTIONS OF THE GOVERNING EQUATIONS

The second term on the right-hand side of Eq. (51) stems from the thermoviscous effect involving the second and third terms as well as the term $\hat{h}\Pi_{xx}\partial_x \ln T$ in Eq. (22). These, together with the second term in Eq. (21), are the terms that do not appear in the Navier-Stokes-Fourier theory. To indicate the difference between the governing equations in the classical Navier-Stokes-Fourier theory and the present theory and to facilitate the solution procedure for Eqs. (50) and (51), we present the governing equations for a one-dimensional shock wave in the former theory

$$\frac{dv}{d\xi}=\frac{3(v^2-v+\theta)}{4\eta^* v}, \tag{52}$$

$$\frac{d\theta}{d\xi}=-\frac{\theta\beta(\alpha+v^2-2v-3\theta)}{5\lambda^*}. \tag{53}$$

These equations follow from Eqs. (50) and (51), if $1-v$ is replaced by ϕ, Eq. (43) is made use of, and the second term on the right-hand side of Eq. (51) is omitted since it arises from the thermoviscous coupling term that must vanish in the linear order. Clearly, Eqs. (52) and (53) are special cases of Eqs. (50) and (51).

We note that in the case of a hard sphere gas the reduced transport coefficients η^* and λ^* depend on θ only:

$$\eta^*=\left(\frac{\theta}{\theta_1}\right)^{1/2},\quad \lambda^*=\left(\frac{\theta}{\theta_1}\right)^{3/2}. \tag{54}$$

To facilitate comparison of the present governing equations with the governing equations in the literature, we note the relation between the reduced distance ξ in the present work with the reduced distance z in the literature:

$$\xi=\frac{x}{l}=z\sqrt{\frac{5\pi}{6}}\,N_M. \tag{55}$$

This relation stems from the difference in the definitions of mean free path in the present work and the literature which has been used to reduce the governing equations. The reduced distance z is defined as $z=x/l_n$ where the mean free path l_n is given by $l_n=(\eta_{01}/\rho_1)\sqrt{\pi/2\mathcal{R}T_1}$. The governing equations (50) and (51) are quite different from the evolution equations for σ and φ appearing in the moment equation approach of Grad [23]. The governing equations in the latter approach, which are differential equations for the stress tensor and heat flux, were found to fail to produce shock solutions for $N_M \geqslant 1.65$. The differential equations for σ and φ arise in the Grad theory, primarily because of the particular closure relations for $\boldsymbol{\psi}_2$ and $\boldsymbol{\psi}_3$ taken, which inevitably give rise to spatial derivatives of $\boldsymbol{\psi}_2$ and $\boldsymbol{\psi}_3$. In the following we examine the governing equations (50) and (51) and the existence of shock solutions with the help of singularities of the direction field equation.

Here we will examine the governing equations in the case of the transport coefficients satisfying Eq. (54). For the Navier-Stokes theory the direction field equation is given by

$$\frac{dv}{d\theta}=\frac{\omega(v^2-v+\theta)}{v(3\theta+2v-v^2-\alpha)}, \tag{56}$$

where

$$\omega=\frac{15\lambda^*}{4\beta\eta^*\theta}. \tag{57}$$

It is independent of θ for the transport coefficients obeying Eq. (54). The singularities of the direction field are given by

$$v^2-v+\theta=0,$$

$$v^2-2v-3\theta+\alpha=0,$$

$$v=0. \tag{58}$$

There are three singular points:

$$P_0: v=\frac{1}{8}(5+\mu),\quad \theta=\frac{1}{64}(15-2\mu-\mu^2),$$

$$P_1: v=\frac{1}{8}(5-\mu),\quad \theta=\frac{1}{64}(15+2\mu-\mu^2),$$

$$P_2: v=0,\quad \theta=0.$$

Note that P_0 and P_1 coincide with the boundary values given in Eqs. (46) and (48). We remark that P_0 and P_1 are also the singular points of the governing equations (52) and (53) for the Navier-Stokes theory where the derivatives $dv/d\xi$ and $d\theta/d\xi$ vanish. It can be shown by calculating the eigenvalues of the linearized governing equations, that P_0 is a saddle point whereas P_1 is a node and P_2 is a spiral. The shock solution is a curve connecting P_0 and P_1 as $\xi\to\infty$ from $\xi=-\infty$. It is possible to show that there exists a unique such solution for every value of α [3,23] since the aforementioned nature of P_0 and P_1 remains invariant for all Mach numbers. Therefore, the Navier-Stokes theory admits shock solutions for all values of Mach number.

We now examine the governing equations (50) and (51) by using the direction field equation

$$\frac{dv}{d\theta}=\frac{-\omega(1-v)(v^2-v+\theta)}{[v(1-v)(v^2-2v-3\theta+\alpha)+3/4\beta(v^2-v+\theta)(\alpha-v^2-5\theta)]}. \tag{59}$$

It is interesting to see that the nonlinear factor $q(\kappa)$ does not appear in this equation and thus the singularities of the direction field is not affected by the nonlinear factor. The singularities of the direction field are given by the equations

$$1-v=0, \tag{60}$$

$$v^2-v+\theta=0, \tag{61}$$

$$v(1-v)(v^2-2v-3\theta+\alpha)+\frac{3}{4\beta}(v^2-v+\theta)(\alpha-v^2-5\theta)=0. \tag{62}$$

The first two equations are for the loci of zero slopes whereas the last equation is for the loci of infinite slopes. Eq. (62) factorizes to the form

$$\frac{15}{4\beta}(\theta-B+\sqrt{B^2+A})(\theta-B-\sqrt{B^2+A})=0, \tag{63}$$

where

$$A=\frac{4\beta}{15}v(v-1)\left[\left(1-\frac{3}{4\beta}\right)\alpha+\left(1+\frac{3}{4\beta}\right)v^2-2v\right], \tag{64}$$

$$B=\frac{2\beta}{5}\left[\left(1-\frac{1}{\beta}\right)v^2-\left(1-\frac{5}{4\beta}\right)v-\frac{3}{4\beta}\alpha\right]. \tag{65}$$

The intersections of the curves arising from Eqs. (60)–(62) are the following five points:

$$P_0: v=\frac{1}{8}(5+\mu), \quad \theta=\frac{1}{64}(15-2\mu-\mu^2),$$

$$P_1: v=\frac{1}{8}(5-\mu), \quad \theta=\frac{1}{64}(15+2\mu-\mu^2),$$

$$P_2 \quad v=0, \quad \theta=0,$$

$$P_3: v=1, \quad \theta=0,$$

$$P_4: v=1, \quad \theta=\frac{1}{5}(\alpha-1).$$

The singularities P_0, P_1, and P_2 coincide with the singularities of the Navier-Stokes equations. It can be shown that P_0 and P_1 are also a saddle point and a node, respectively, whereas P_2 is a spiral as in the case of Navier-Stokes theory. An example of loci of zero and infinite slopes for both the Navier-Stokes and present theories are plotted in the case of $N_M=2$ in Fig. 1, where the broken line is for the Navier-Stokes theory and the heavy solid line is for both the Navier-Stokes and present theories, whereas the light line is for the present theory only. The light line is a closed loop. The point P_2 is located at the origin of the (v,θ) coordinates, whereas points P_3 and P_4 are the intersection of the closed loop with line $v=1$. Both theories share the same inverted parabola (heavy line) which intersects the broken line and the closed loop described by Eq. (62) or Eq. (63) at the same points P_0 and P_1. Point P_3 is neutral in a direction and unstable in the other, whereas P_4 is unstable—an unstable focus. It therefore means that both theories not only share the same boundary conditions at the upstream and downstream, but also have an intersection of domains which are bounded by curves of negative slopes and where the shock solutions lie. Singularities P_3 and P_4 are not associated with shock solutions. It must be noted that line $v=0$ is neither the locus of zero slopes nor the locus of infinite slopes. As the Mach number increases, the intersections P_0, P_3, and P_4 coalesce at $v=1$ which corresponds to the boundary value for velocity at infinite Mach number. This situation is almost achieved at $N_M=10$ as shown in Fig. 2. The shock solution must connect P_0 and P_1. The fact that the singularities P_0 and P_1 are shared by both theories and there is an intersection of domains where the slopes are negative means that a shock solution must exist for the governing equations (50) and (51) for all Mach numbers as is the case for the Navier-Stokes equations for all Mach numbers. The uniqueness follows from the uniqueness of the solution to Eq. (59).

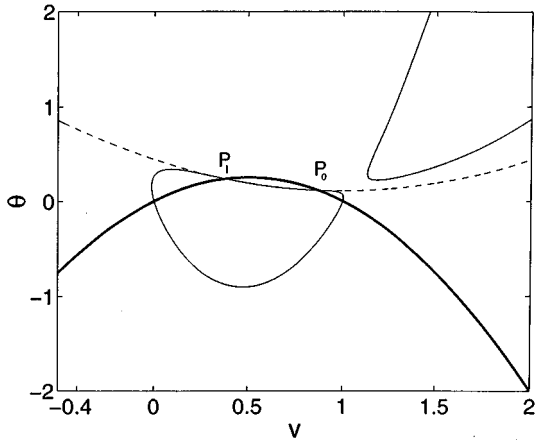

FIG. 1. Loci of zero and infinite slopes in the direction field for the Navier-Stokes and generalized hydrodynamic theories in the case of $N_M=2$. The broken line is for the Navier-Stokes theory whereas the heavy line is for both the Navier-Stokes and present theories. The light lines are for the present theory which predicts a closed loop for a locus. Both theories share the same points of intersection P_0 and P_1 as well as P_2 and the domain of negative slopes bounded by curves passing through P_0 and P_1. Shock solutions lie in the domain and connect P_0 and P_1. Points P_2 and P_3, which are intersections of the closed loop and the bold solid line, and P_4, which is the intersection of the closed loop and line $v=1$, are not indicated in the figure. One of the parabolas which should appear in the the upper left corner is out of the picture in the present figure.

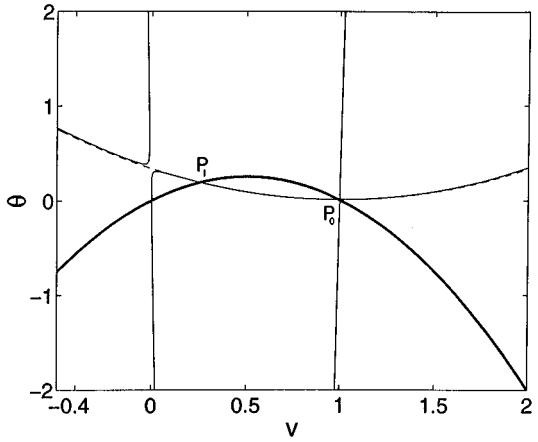

FIG. 2. Same as Fig. 1 except for $N_M=10$. Notice that P_0 already has almost approached point P_3 at $v=1$, $\theta=0$. The closed loop in Fig. 1 becomes almost rectangular with the minimum at about $\theta\approx-50$. The parabola at the upper right corner almost meets with the closed loop at $v=1$ and $\theta=0$.

IV. NUMERICAL RESULTS AND COMPARISON WITH SIMULATION DATA

A. Shock profiles and widths

The governing equations are numerically solved subject to the boundary conditions given in Eqs. (50) and (51). Some examples for shock profiles for velocity and density are given for a few values of Mach number in Figs. 3 and 4. In these and other figures in this work, the solid line is for $N_M=1.5$, the bold solid line is for $N_M=2$, the dashed line is for $N_M=5$, the dotted line is for $N_M=8$, and the dash-dotted line is for $N_M=10$. The corresponding values for the stress (σ) and heat flux (φ) are plotted in Fig. 5. In the literature, the shock width δ is defined by means of the density profile in the following form:

$$\delta=\frac{n_2-n_1}{(dn/dz)_{\max}}, \tag{66}$$

where the reduced distance z has the relation to the reduced

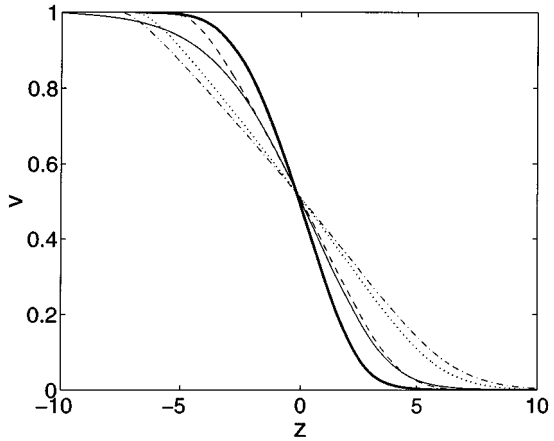

FIG. 3. Shock profiles for velocity for various Mach numbers for a Maxwell gas. Solid line: $N_M=1.5$; bold solid line: $N_M=2$; dashed line: $N_M=5$; dotted line: $N_M=8$; dash-dotted line: $N_M=10$.

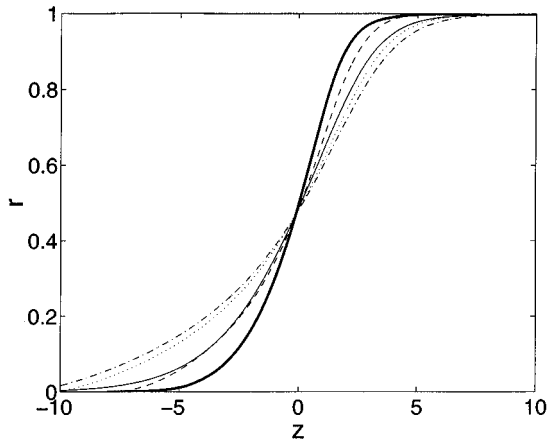

FIG. 4. Shock profiles for density for various Mach numbers for a Maxwell gas. The same meanings for the lines as in Fig. 3.

distance ξ used in this work; see Eq. (55). In Fig. 6 the shock widths calculated ($\bigcirc$) by the present theory are compared with Monte Carlo simulation data ($*$) by Nanbu and Watanabe [5], the results by the Mott-Smith C_x^2 ($+$) and C_x^3 ($\square$) closures [14], and the results by Salwen *et al.* who modified the Mott-Smith method to include an additional moment [e.g., (C_x^2,C_xC^2) ($\times$) or (C_x^3,C_xC^2) ($\diamond$) closures] [16]. The solid line is drawn through the results of the present theory to guide the eyes. The Navier-Stokes predictions are presented

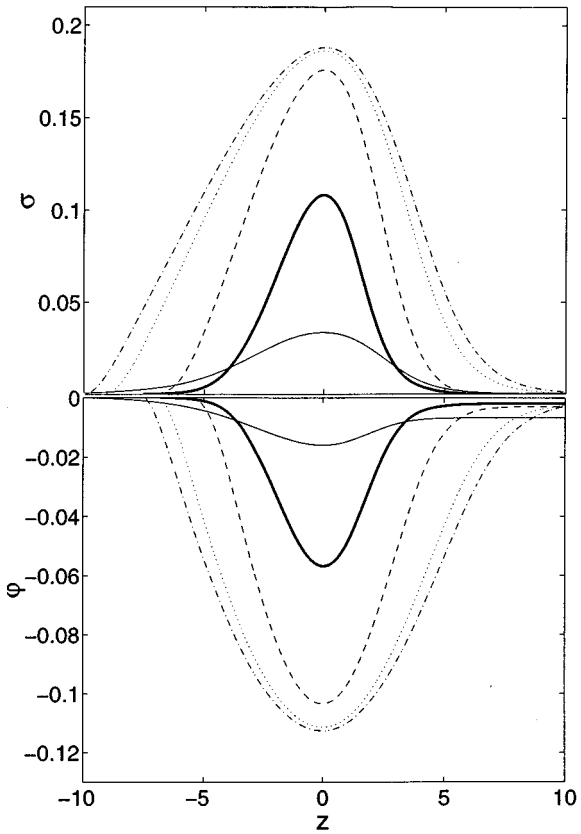

FIG. 5. Shock profiles for stress and heat flux for various Mach numbers for a Maxwell gas. The same meanings for the lines as in Fig. 3.

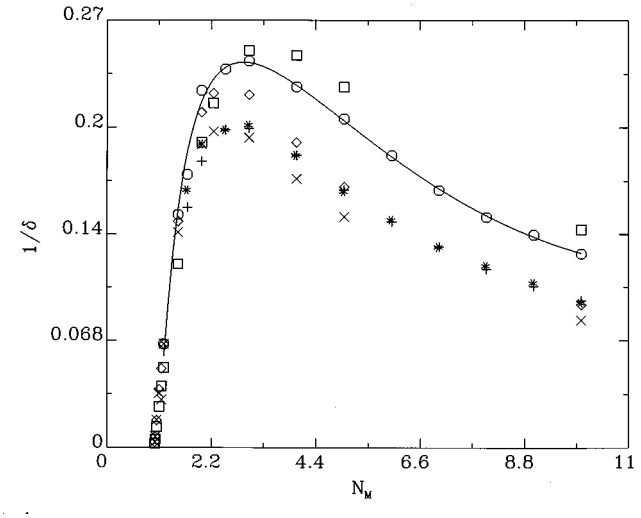

FIG. 6. Inverse shock width vs N_M for a Maxwell gas. The solid line is drawn through the present results to guide the eyes. The meanings of the symbols are as follows: ○: present result; ∗: Monte Carlo result of Nanbu and Watanabe [5]; +: Mott-Smith C_x^2 closure [5]; □: Mott-Smith C_x^3 closure [16]; ×: Mott-Smith (C_x^2, C_xC^2) closure [16]; ◇: Mott-Smith (C_c^3, C_xC^2) closure [16].

in Table I together with the inverse shock width values for the points appearing in Fig. 6. Since the differential equations (50) and (51) are stiff, the solutions are obtained by using Gear's method with a relatively high tolerance ($<10^{-4}$). Therefore, the numerical results are not of high precision, but they are adequate for comparison. The present results obtained are closer to those by the Mott-Smith C_x^3 closure (□) for all Mach numbers examined whereas they differ from the Monte Carlo simulation data (∗) of Nanbu and Watanabe by 14 to 20 %. Note that the Monte Carlo simulation results well agree with the results by the Mott-Smith C_x^2 closure (+), but this method of closure does not give results convergent with those by the Mott-Smith C_x^3 closure (□). The Monte Carlo simulation method of Nanbu and Watanabe [5] is a modification of Bird's method [4] and, especially, its treatment of collisions is basically the same as in the latter method. Consequently, the method of Nanbu and Watanabe, as expected and noted by them [5], gives the same results as by the Bird method. Since the Mott-Smith method can be by no means regarded as exact and the C_x^2 and C_x^3 closures give divergent results, the converged results are quite probably located elsewhere if the method ever yields convergent results as the number of moments included is increased. The reason for this expectation can be seen in the work of Salwen *et al.* [16] which gives different values from those by the Mott-Smith C_x^2 closure for the inverse shock width. Interestingly, the Mott-Smith C_x^2 closure method yields the shock widths which coincide with the results obtained by the Monte Carlo simulation method of Nanbu and Watanabe [5], who report that the same results also are obtained by the method of Bird [4]. Since the simulation results by Yen and Ng [7] differ from those of Nanbu and Watanabe, it is not clear where true values lie. The comparison made in Fig. 6 therefore does not resolve the question regarding the accuracy and reliability of the present continuum theory method, although it produces results that appear to have a qualitatively correct behavior with regard to the Mach number dependence in the entire regime of Mach number.

To resolve this question, we have performed a calculation with a variable hard sphere model which gives the viscosity as $\eta_0 = \mu_0 (T/T_0)^s$, where μ_0 and T_0 are constants and we have taken $s = 0.75$ in this work. This value of s lies between 0.72 for the shock tube value and 0.81 for the wind tunnel value suggested in Ref. [6]. This model has been tested in connection with shock widths for argon and helium [6]. To make a comparison of the results by the formulas in the present theory with experiment it is necessary to use a somewhat different length scale from the scale given in Eq. (55). This difference arises from the different definitions of mean free path. The experimental data in question are based on the definition of mean free path by Bird [38] l_B

TABLE I. Inverse shock widths by various theories for a Maxwell gas. M-S_2: Mott-Smith C_x^2 closure, M-S_3: Mott-Smith C_x^3 closure [14]; SGZ_{23}: Salwen, Grosch, Ziering (C_x^2, C_xC^2) closure, SGZ_{33}: Salwen, Grosch, Ziering (C_x^3, C_xC^2) closure [16]; MC: Monte Carlo [5]; NS: Navier-Stokes.

N_M	M-S_2	M-S_3	SGZ_{23}	SGZ_{33}	MC	Present	NS
1.2	0.0557	0.0504	0.0653	0.0650		0.0651	
1.5	0.124	0.116	0.136	0.143		0.147	
1.7	0.152[a]				0.164	0.173	0.188
2	0.184	0.193	0.192	0.212	0.193	0.226	0.232
2.25	0.198	0.218	0.200	0.224			
2.5	0.201[a]				0.202	0.239	0.275
3	0.206	0.251	0.196	0.223	0.205	0.244	0.293
4	0.188	0.248	0.170	0.193	0.186	0.228	
5	0.165	0.228	0.146	0.165	0.163	0.208	
6	0.143[a]				0.145	0.185	
7	0.127[a]				0.128	0.163	
8	0.113[a]				0.116	0.146	
9	0.102[a]				0.105	0.135	
10	0.0945	0.138	0.0804	0.0902	0.0925	0.123	

[a]Data from Ref. [5].

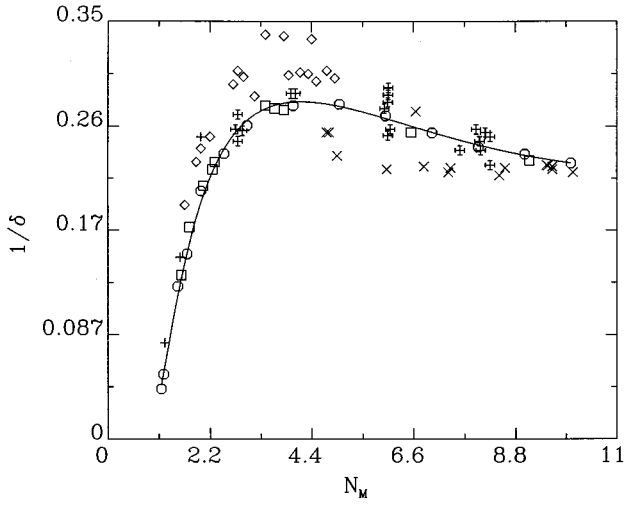

FIG. 7. Comparison of theoretical inverse shock widths with experimental data at various Mach numbers. A variable hard-sphere model is used for the potential for which $\eta_0=\mu_0(T/T_0)^s$ with $s=0.75$. ⬭: present theory, □: Alsmeyer [39], ✠: Schmidt [40], +: Garen *et al.* [41], ◇: Linzer and Hornig [42], and ×: Camac [43]. A solid line is drawn through the theoretical values to guide the eyes.

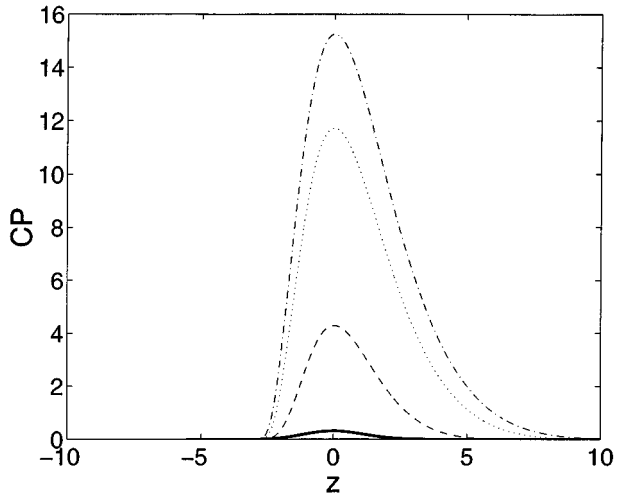

FIG. 8. Profiles for reduced calortropy production for various Mach numbers for a Maxwell gas. The same meanings for the lines as in Fig. 3. The case for $N_M=1.5$ is invisible in the scale of the figure.

$=(\eta_{01}/\rho_1)B\sqrt{\pi/2\mathcal{R}T_1}$ where $B=(7-2s)(5-2s)/24$. For this definition of mean free path the reduced distance ξ in the present theory is related to the reduced distance used for the experimental data considered here as follows:

$$\zeta=zB\sqrt{\frac{5\pi}{6}}\,N_M. \tag{67}$$

Therefore, the shock widths are calculated with the formula

$$\delta=B\sqrt{\frac{5\pi}{6}}\,N_M\,\frac{n_2-n_1}{(dn/d\xi)_{\max}}. \tag{68}$$

The results calculated (⬭) for the variable hard-sphere model are compared with various experimental data reported by Alsmeyer [39] (□), Schmidt [40] (✠), Garen *et al.* [41] (+), Linzer and Hornig [42] (◇), and Camac [43] (×) in Fig. 7. A line is drawn through the theoretical values in order to guide the eyes. Although the data of Linzer and Hornig and Camac do not appear to be consistent with the data of Alsmeyer, Schmidt, and Garen *et al.* and therefore are difficult to analyze with the present theory together with those of the latter, they are included in the figure for completeness. Given the experimental uncertainties (4–5 % according to Alsmeyer) and the errors in the numerical solutions of the governing equations, the theoretical results are judged to be in good agreement with experiment and, especially, with those by Alsmeyer, Schmidt, and Garen *et al.* In fact, the agreement with Alsmeyer's data is excellent. Therefore, it can be concluded that the present theory yields reliable results for inverse shock widths over the entire experimental range of Mach number.

The present theory is a continuum hydrodynamic theory for shock waves, and it provides shock structures adequately for the range of Mach number studied by other methods and by experiments. This is in contrast to the Navier-Stokes theory and other approaches [23–25] in the moment method mentioned earlier. As far as the present authors are aware, there is no continuum hydrodynamic theory to have accomplished such results comparable with experiments over the entire range of Mach number studied. We thus have achieved an adequate continuum theory generalization of the Navier-Stokes theory for shock waves in the hypersonic regime, and the closure relations, together with the nonlinear factor $q(\kappa)$, taken for the constitutive equations for the stress tensor and heat flux hold the key to the results obtained.

B. Calortropy production—energy dissipation

Energy dissipation is closely associated with shock wave phenomena. It competes with compression in determining the thickness of a shock wave. Therefore, it is interesting to examine energy dissipation [44]. In the framework of irreversible thermodynamics on which the present theory is based, the calortropy production [30] gives a measure of energy dissipation in the system from a useful to less useful form. We have calculated the calortropy production associated with shock waves for various Mach numbers. For the constitutive equations the calortropy production is given by [27]

$$\sigma_{\rm cal}=k_B g\,\kappa(\mathbf{\Pi},\mathbf{Q})\sinh\kappa(\mathbf{\Pi},\mathbf{Q}), \tag{69}$$

where $g=(m/k_BT)^{1/2}/2n^2d^2$. Therefore a reduced calortropy production relative to the upstream condition may be defined by

$$\hat{\sigma}_{\rm cal}=\sigma_{\rm cal}/k_Bg(T_1,n_1)=\sqrt{\frac{\theta}{\theta_1}}\left(\frac{r_1}{r}\right)^2\kappa(\sigma,\varphi)\sinh\kappa(\sigma,\varphi). \tag{70}$$

The reduced calortropy production is computed from the shock solutions obtained and presented in Fig. 8. It is peaked around the transition point in the shock profile and the peak

height increases with the Mach number. In the scale of the figure $\hat{\sigma}_{\rm cal}$ is so small for $N_M=1.5$ that it does not show up in the figure.

Since the global value for calortropy production is of interest and perhaps more relevant to the present problem, we define a reduced integral calortropy production

$$\Xi_c=\int_{-\infty}^{\infty}d\xi\sqrt{\frac{\theta}{\theta_1}}\left(\frac{r_1}{r}\right)^2\kappa(\sigma,\varphi)\sinh\kappa(\sigma,\varphi)$$
$$=\sqrt{\frac{5\pi}{6}}\,N_M\int_{-\infty}^{\infty}dz\sqrt{\frac{\theta}{\theta_1}}\left(\frac{v}{v_1}\right)^2\kappa(\sigma,\varphi)\sinh\kappa(\sigma,\varphi). \tag{71}$$

This global calortropy production has been calculated as a function of Mach number in the case of the Maxwell model. The results of the calculation show that Ξ_c increases with Mach number as $(N_M-a)^\alpha$; namely,

$$\Xi_c=K(N_M-a)^\alpha, \tag{72}$$

where K, a, and α are constant parameters. For the Maxwell model $a\simeq 0.85$ and $\alpha\simeq 3.14$, whereas $a\simeq 0.87$ and $\alpha\simeq 2.98$ for the variable hard sphere model with $s=0.75$. It probably is fair to take $\alpha=3.0$ as an approximation, given the uncertainties of the numerical results and curve fittings. This energy dissipation competes with the compressional effect of shock in determining the shock thickness.

V. DISCUSSION AND CONCLUSION

In this paper we have presented a continuum hydrodynamic theory of shock waves which yields shock structures (shock widths) comparable to those by Monte Carlo methods and the Mott-Smith methods over the entire range of Mach numbers studied for the Maxwell model of potential. It removes the weakness of the Navier-Stokes theory of shock waves. However, the present results agree only within 14–20 % with the Monte Carlo results obtained by Nanbu and Watanabe [5] and with the results by the Mott-Smith C_x^2 closure method. Our present results are closer in performance to those by the Mott-Smith C_x^3 closure method. Since none of the Mott-Smith methods can be judged to be exact and they yield nonconvergent numerical results for the inverse shock widths for the Maxwell model, it is difficult to conclude which one is closer to the true values for shock widths. To resolve this question, we have computed the inverse shock widths by the present theory for a variable hard sphere model and compared the results with experimental data on argon. They are found to be in good agreement with experiments. Thus, we now have a continuum hydrodynamic theory for shock waves which correctly performs beyond the regime of Mach number where the classical Navier-Stokes theory remains useful. Such a theory is designed from the moment equations derived from the Boltzmann kinetic equation, primarily, by using different closures from those used in the moment methods by others for the same purpose. The performance of the governing equations is enhanced by the presence of the nonlinear factor $q(\kappa)$ which basically arises on resummation of the Boltzmann collision contributions for all Knudsen numbers. The present theory is thermodynamically consistent in the sense that it conforms to the requirement of thermodynamic laws. The aforementioned nonlinear factor is known to be responsible for correctly accounting for the shear rate dependence of fluids in the non-Newtonian regime of viscosity [31–36], the emergence [45] of boundary layers in flows under a steep pressure gradient, plug flows [46,47], the resolution [48] of the Knudsen paradox [49], etc. The nonlinear factor $q(\kappa)$ is not present in the moment equations in the conventional approach following the formulation of Grad's moment method. As is evident from Eq. (70), $q(\kappa)$ is closely related to the calortropy production arising from the irreversible process in the system since Eq. (70) can be recast in the form

$$\sigma_{\rm cal}=k_B g\kappa^2(\mathbf{\Pi},\mathbf{Q})q(\kappa)\geqslant 0. \tag{73}$$

Since $\kappa^2(\mathbf{\Pi},\mathbf{Q})$ is basically the Rayleigh dissipation function, this nonlinear factor $q(\kappa)$ modifies the Rayleigh dissipation function [50] because there are nonlinear transport processes present in the system.

The generalized hydrodynamic equations presented in this work have been derived from the Boltzmann equation for dilute gases. Therefore, one may infer that they are limited to such gases. However, it is shown in the literature [27] that essentially the same forms of evolution equations hold for liquids and for dense gases except for the meanings of the parameters appearing in the equations which must be regarded as those for liquids or dense gases. More specifically, one can simply regard the transport coefficients η_0 and λ_0 as well as p and $\hat{C}_p$ in the constitutive equations (19) and (20) as those for the liquid or dense gas in question and apply them to flow problems in such fluids. Therefore, the good agreement of the theoretical results with experiments suggests the utility of the present generalized hydrodynamics approach to shock wave phenomena in liquids or dense gases where Monte Carlo simulation methods comparable to those of Bird and Nanbu and Watanabe are not available at present. In this connection, we note that there are some molecular dynamics simulations on shock waves in liquids [8–10]. In conclusion, we believe that, together with the conservation laws for mass, momentum, and energy, the constitutive equations for $\mathbf{\Pi}$ and $\mathbf{Q}$ presented in this work form a continuum (generalized hydrodynamic) theory of flow phenomena including shock waves.

Finally, we would like to add a note in connection with the closure relations leading to Eqs. (19) and (20), which arise in the adiabatic approximation. Instead of the closure relations in Eq. (10), one may treat $\rho d\hat{\mathbf{\Pi}}/dt+\nabla\cdot\psi_2$ and $\rho d\hat{\mathbf{Q}}/dt+\nabla\cdot\psi_3$ as a perturbation in Eqs. (5) and (6), respectively. Then, the steady-state constitutive equations (19) and (20) arise as the lowest-order approximations to Eqs. (5) and (6) in the perturbation theory applied to the generalized hydrodynamic equations within the framework of the first thirteen moments.

ACKNOWLEDGMENTS

The present work has been supported in part by a grant from the Natural Sciences and Engineering Research Council of Canada.

[1] R. Becker, Z. Phys. **8**, 321 (1922).
[2] L. H. Thomas, J. Chem. Phys. **12**, 449 (1944).
[3] D. Gilbarg and D. Paolucci, J. Rat. Mech. Anal. **2**, 617 (1953).
[4] G. Bird, *Molecular Gas Dynamics* (Clarendon, Oxford, 1976).
[5] K. Nanbu and Y. Watanabe, report of the Institute of High Speed Mechanics, Tohoku University, Japan, 1984, Vol. 48.
[6] G. C. Pham-van-Diep, D. A. Erwin, and E. P. Muntz, J. Fluid Mech. **232**, 403 (1991); D. A. Erwin, G. C. Pham-van-Diep, and E. P. Muntz, Phys. Fluids A **3**, 697 (1991).
[7] S. Yen and W. Ng, J. Fluid Mech. **65**, 127 (1974).
[8] W. G. Hoover, Phys. Rev. Lett. **42**, 1531 (1979).
[9] B. L. Holian, W. G. Hoover, B. Moran, and G. K. Straub, Phys. Rev. A **22**, 2798 (1980).
[10] B. L. Holian, Phys. Rev. A **37**, 2562 (1988); B. L. Holian, C. W. Patterson, M. Mareschal, and E. Salomons, Phys. Rev. E **47**, R24 (1993).
[11] C. S. Wang Chang and G. E. Uhlenbeck, in *Studies in Statistical Mechanics*, edited by J. De Boer and G. E. Uhlenbeck (North-Holland, Amsterdam, 1970), Vol. 5.
[12] J. D. Foch, Jr. and G. W. Ford, in *Studies in Statistical Mechanics* (Ref. [11]).
[13] K. A. Fiscko and D. R. Chapman, Prog. Aeronaut. Astronaut. **118**, 374 (1989).
[14] H. M. Mott-Smith, Phys. Rev. **82**, 885 (1951).
[15] C. Muckenfuss, Phys. Fluids **5**, 1325 (1962).
[16] H. Salwen, C. E. Grosch, and S. Ziering, Phys. Fluids **7**, 180 (1964).
[17] M. T. Chahine and R. Narashimha, Adv. Appl. Mech. **1**, Suppl. 3, 140 (1965).
[18] L. H. Holway, Adv. Appl. Mech. **1**, Suppl. 3, 193 (1965).
[19] M. N. Kogan, *Rarefied Gas Dynamics* (Plenum, New York, 1967).
[20] S. M. Deshpande and R. Narashimha, J. Fluid Mech. **36**, 545 (1969).
[21] R. Narasimha and P. Das, Philos. Trans. R. Soc. London, Ser. A **330**, 217 (1990).
[22] A. G. Bashkirov and A. V. Orlov, Phys. Rev. E **53**, R17 (1996).
[23] H. Grad, Commun. Pure Appl. Math. **5**, 257 (1952).
[24] L. H. Holway, Phys. Fluids **7**, 911 (1964).
[25] A. M. Anile and A. Majorana, Meccanica **16**, 149 (1982).
[26] W. Weiss, Phys. Rev. E **52**, R5760 (1995).
[27] B. C. Eu, *Kinetic Theory and Irreversible Thermodynamics* (Wiley, New York, 1992).
[28] S. R. de Groot and P. Mazur, *Nonequilibrium Thermodynamics* (North-Holland, Amsterdam, 1962).
[29] B. C. Eu, J. Chem. Phys. **103**, 10 652 (1995).
[30] B. C. Eu, Phys. Rev. E **51**, 768 (1995).
[31] B. C. Eu, Phys. Lett. **96A**, 29 (1983); J. Chem. Phys. **79**, 2315 (1983).
[32] Y. G. Ohr and B. C. Eu, Phys. Lett. **101A**, 338 (1984).
[33] B. C. Eu and Y. G. Ohr, J. Chem. Phys. **81**, 2756 (1984).
[34] B. C. Eu and R. E. Khayat, Rheol. Acta **30**, 204 (1991).
[35] K. Mao and B. C. Eu, Phys. Rev. A **48**, 2471 (1993).
[36] D. K. Bhattacharya and B. C. Eu, Mol. Phys. **59**, 1145 (1986); Phys. Rev. A **35**, 4850 (1987).
[37] S. Chapman and T. G. Cowling, *The Mathematical Theory of Nonuniform Gases*, 3rd ed. (Cambridge, London, 1970).
[38] G. A. Bird, Phys. Fluids **26**, 3222 (1983).
[39] H. Alsmeyer, J. Fluid Mech. **74**, 497 (1976).
[40] B. Schmidt, J. Fluid Mech. **39**, 361 (1969).
[41] W. Garen, R. Synofzik, and A. Frohn, A. Inst. Astronaut. Aeronaut. J. **12**, 1132 (1974).
[42] M. Linzer and D. F. Hornig, Phys. Fluids **6**, 1661 (1963).
[43] M. Camac, Adv. Appl. Mech. **1**, 240 (1965).
[44] In this connection, we note that Hosogawa and Inage used the steady-state Boltzmann entropy balance equation to calculate shock widths and the Boltzmann entropy production. See I. Hosogawa and S. Inage, J. Phys. Soc. Jpn. **55**, 3402 (1986). In this paper, the authors choose an approximate bimodal distribution function such that the steady-state Boltzmann entropy balance equation is satisfied as closely as possible. Nevertheless, the method is not quite a variational principle.
[45] B. C. Eu, Phys. Rev. A **36**, 400 (1987).
[46] B. C. Eu, Phys. Rev. A **77**, 4504 (1988).
[47] B. C. Eu, Am. J. Phys. **58**, 83 (1990).
[48] B. C. Eu, Phys. Rev. A **40**, 6395 (1989).
[49] M. Knudsen, Ann. Phys. (N.Y.) **28**, 75 (1909).
[50] Lord Rayleigh, *Theory of Sound* (Dover, New York, 1945).